AQPs enhance salinity tolerance in *Melilotus albus* through oxidative damage mitigation and osmotic adjustment

Zhenjie Xie[1], Xifang Zong[1], Caibin Zhang[1], Jiyu Zhang*

State Key Laboratory of Herbage Improvement and Grassland Agro-ecosystems; College of Pastoral Agriculture Science and Technology, Lanzhou University, Lanzhou, 730020, P. R. China

[1] These authors contributed equally to this work.
*** Corresponding author.**
***E-mail address*: zhangjy@lzu.edu.cn (J. Zhang)**

Abstract

Soil salinity is a major environmental factor limiting global agricultural productivity. Elucidating plant responses to salt stress is crucial for developing resilient crops. *Melilotus albus*, a vital forage and green manure crop renowned for strong salinity tolerance, is an ideal candidate for investigating salt response mechanisms. Aquaporins (AQPs), integral membrane channels involved in cellular water regulation, are considered key components in plant responses to environmental stresses. In present study, 44 *MaAQP* genes were identified in the *M. albus* genome and grouped into five categories: *PIP*, *TIP*, *NIP*, *SIP* and *XIP*. Comparative analysis revealed that genes within the same subfamily share similar structures, with the NPA motif and ar/R filter sequence being highly conserved in the *PIP* subfamily. Transcriptome profiling combined with qRT-PCR validation revealed that *MaAQP* responds to developmental cues, abiotic stress conditions, and ABA signaling pathways. Overexpression experiments in both yeast and root hair transformation systems showed that *MaPIP2;1*, *MaTIP2;2*, and *MaPIP1;1* enhanced salt tolerance. In transgenic hairy roots, these genes alleviated oxidative damage by reducing MDA content and enhanced osmotic adjustment through increased proline and soluble sugar levels. These results highlight the functional significance of the *MaAQP* family salinity adaptation and identify promising targets for enhancing stress resilience in forage and crop breeding.

Keywords: *Melilotus albus*; aquaporins (AQPs); salt tolerance; osmotic adjustment

1. Introduction

Soil salinity is one of the most critical abiotic stresses limiting global agricultural productivity and threatens the sustainability of crop and forage production worldwide (Zhao et al., 2020). Enhancing salt tolerance in economically and ecologically important plant species is therefore a key goal in sustainable agriculture (Zhang et al., 2022). *Melilotus albus*, a salt-tolerant legume widely distributed across various

regions of the world, has been extensively utilized in saline soil remediation, forage production, and green manure (Rogers et al., 2008). Due to its remarkable adaptability to saline-alkali soils, *M. albus* represents an ideal candidate for investigating salt tolerance in legumes.

Among the critical factors influencing plant responses to salinity, the regulation of water transport plays a particularly crucial role, as salt stress frequently induces osmotic imbalance and disrupts water uptake. Aquaporins (AQPs), which are membrane-bound proteins that aid in the transport of water and other small solutes, are essential for maintaining water balance under these conditions (Chrispeels and Maurel, 1994; Javot and Maurel, 2002).

AQPs are typically membrane proteins with a molecular weight around 30 kDa and belong to the Major Intrinsic Protein (MIP) superfamily. They feature a conserved "hourglass" shape consisting of six transmembrane α-helices and two distinctive NPA (Asn-Pro-Ala) motifs in loops B and E, which are essential for selective water transport (Walz et al., 1997; Johansson et al., 2001; Maurel et al., 2008). Based on amino acid sequence similarity, AQPs in higher plants can be classified into four major subfamilies: PIP, TIP, NIP, and SIP (Johanson et al., 2001). Additionally, an unclassified subfamily, XIP is found in certain dicots, such as *Medicago truncatula* (Min et al., 2019). Among them, PIP and TIP are the most widely distributed AQPs on the plasma membrane and tonoplast and are considered to play crucial functional roles. (Kadam et al., 2017; Reddy et al., 2017).

Research has shown that salt stress can influence AQP gene expression, usually leading to an initial suppression of expression to reduce water loss, followed by an increase in expression during prolonged or high salt conditions to help reestablish water balance. In *Arabidopsis thaliana*, *Oryza sativa*, and *Hordeum vulgare*, *AQP* expression is tightly linked to hydraulic conductivity and stress resilience (Kawasaki et al., 2001; Maathuis et al., 2003; Zhang et al., 2017). However, the functional roles and expression dynamics of *AQP* in *M. albus* under salinity remain poorly understood. The present study focused on a comprehensive identification of the *AQP* gene family in *M. albus*, examined the expression profiles of these genes, and assessed the functional contributions of specific *AQP* members in response to saline stress using yeast expression systems and root hair transformation techniques. These findings will provide new insights into the molecular basis of salt tolerance and contribute to the development of stress-resilient forage and legume crops.

2. Materials and methods

2.1. Identification and sequence analysis of MaAQP genes

The genome sequence of *M. albus* was previously sequenced by our research group (NCBI BioProject ID: PRJNA647665) (Wu et al., 2022). The AQP protein sequences from *Arabidopsis thaliana* and *Medicago truncatula* were retrieved from the Phytozome database. These sequences were then used by BLASTP to identify homologous sequences in the *M. albus* genome. The AQP family members were predicted to contain only the MIP domain (PF00230), determined via sequence analysis using Hidden Markov Models from the Pfam database. The physicochemical properties of MaAQP proteins were predicted using ExPasy ProtParam. Subcellular localization was predicted using Plant-mPLoc and WoLF PSORT.

2.2. Phylogenetic analysis and subfamily classification of MaAQP proteins

Sequence alignments were conducted using Clustal W, and a neighbor-joining phylogenetic tree was built with MEGA7 software, utilizing 1,000 bootstrap replicates. The MaAQP proteins were grouped into subfamilies based on their clustering with homologous proteins from *Arabidopsis thaliana* and *Medicago truncatula*.

2.3. Gene structure and conserved motif analysis

Conserved motifs in MaAQP proteins were identified through the MEME Suite, with the motif count limited to 20. The gene structures were visualized using TBtools, based on GFF3 annotation files, illustrating exon-intron arrangements.

2.4. Chromosomal distribution, gene duplication, and Ka/Ks analysis

The chromosomal locations and syntenic relationships of MaAQP genes were examined with TBtools. Gene duplication events were identified using OrthoMCL v5, and Ka/Ks determined with PAML's yn00 NG model to assess selection pressure.

2.5. Cis-acting regulatory element analysis of promoter regions

The 2000 bp upstream promoter sequences of *MaAQP* genes were extracted and submitted to the PlantCARE database to identify cis-acting elements.

2.6. Transcriptome-based expression profiling

M. albus was cultivated in vermiculite under controlled environmental conditions. One-month-old seedlings underwent treatment with 250 mM NaCl, 20% PEG-6000, or 100 mM ABA. Samples (roots and shoots) were collected at 0 h, 3 h, and 24 h for transcriptome sequencing. Tissue samples from roots, stems, leaves, and flowers were harvested during the flowering period. Gene expression levels were quantified using StringTie, and FPKM values were calculated. Heatmaps and Venn diagrams were used

to assess expression patterns and stress responses (Chen et al., 2023).

2.7. Quantitative real-time PCR analysis

RNA was isolated with a commercial extraction kit (Tiangen), and cDNA synthesis was carried out using the FastKing protocol. Primer design was completed with PerlPrimer v1.1.21 (Table S1). Quantitative PCR was performed on the CFX96 platform with SYBR Green qPCR reagents. *β*-tubulin acted as a reference gene, and transcript levels were assessed using the 2^−ΔΔCT approach.

2.8. Heterologous expression of MaAQP genes in yeast

The complete coding regions of *MaPIP2;1*, *MaTIP2;2*, and *MaPIP1;1* were generated with fusion primers designed by SnapGene (Table S1) and HS High-Fidelity DNA Polymerase. Amplified products were inserted into the pYES2 system and introduced into INVSc1 yeast cells via lithium acetate transformation (Wei et al., 2019). Transformed yeasts were first grown in SC-U medium containing 2% glucose, then transferred to 2% galactose-containing SC-U medium for induction. Cell suspensions were adjusted to OD600 = 1.0, serially diluted, and exposed to 5 M NaCl for stress assays. Cultures were adjusted to OD600 = 1.0, serially diluted, and plated under 5 M NaCl. Growth was observed after 36-48 h.

2.9. Hairy root transformation, expression analysis, and physiological assays in M. albus

Hairy root transformation followed the protocol of Wang et al (2021). *M. albus* seeds (JiMa49) were sterilized, vernalized, and germinated. Hypocotyls were inoculated with *Agrobacterium rhizogenes* and cultured on half-strength MS medium. After root development, transgenic roots were confirmed by qRT-PCR, 250 mM NaCl was applied for a 3-day stress treatment.

Roots were flash-frozen for physiological assays. MDA, proline, and soluble sugar contents were quantified using the TBA method, ninhydrin assay, and anthrone method, respectively. All experiments included three biological and three technical replicates.

2.10. Data analysis and statistics

All experiments included at least six independent biological replicates. Statistical differences were assessed using Tukey's honestly significant difference (HSD) test following ANOVA ($P < 0.05$). Data visualization was performed with Origin 2024.

3. Results

3.1. Identification and phylogenetic analysis of MaAQP family

A total of 44 *MaAQP* genes were discovered in the *M. albus* genome and named according to

123 previous studies (Table S2). To investigate the evolutionary lineage between MaAQP and the AQP
124 families of *A. thaliana* and *M. truncatula*, a phylogenetic comparison was performed. This analysis
125 allowed classification of MaAQP proteins into five distinct subfamilies: PIP, TIP, NIP, SIP, and XIP,
126 comprising 2, 5, 7, 2, and 1 subtypes, and 10, 12, 16, 4, and 2 members respectively (Fig. 1).
127 The properties of MaAQP proteins were further analyzed. 44 MaAQP proteins ranged from 239
128 (MaSIP2;1) to 808 (MaNIP7;1) amino acid residues, with a mean of 294.1 amino acids, and 95.5% (42/44)
129 MaAQP proteins ranged from 239 to 330 amino acids in length, showing minor variation. The relative
130 molecular weights (Mws) ranged from 25.0 (MaSIP2;1) to 89.8 (MaNIP7;1) kDa, with the average being
131 31.3 kDa. The proteins exhibited a wide range of isoelectric points (pI), from 5.03 (MaTIP2;3) to 9.97
132 (MaSIP1;3). Out of the total, 27 proteins had pI values above 7, while the remaining 17 displayed values
133 equal to or below this threshold (Table S2). The hydropathy index (GRAVY) also varied considerably,
134 ranging between -0.232 (MaPIP1;5) and 0.973 (MaTIP2;1), indicating a broad spectrum of hydrophilic
135 and hydrophobic properties among the proteins. Subcellular localization predictions were made using
136 Plant-mPLoc and WoLF PSORT, which showed consistent results for 86.4% (38 of 44) of the proteins.
137 Among the 38 MaAQP proteins with consistent prediction, all TIP subfamily proteins were anchored in
138 the vacuolar membrane, while other subgroup proteins were targeted the plasma membrane (Table S2).

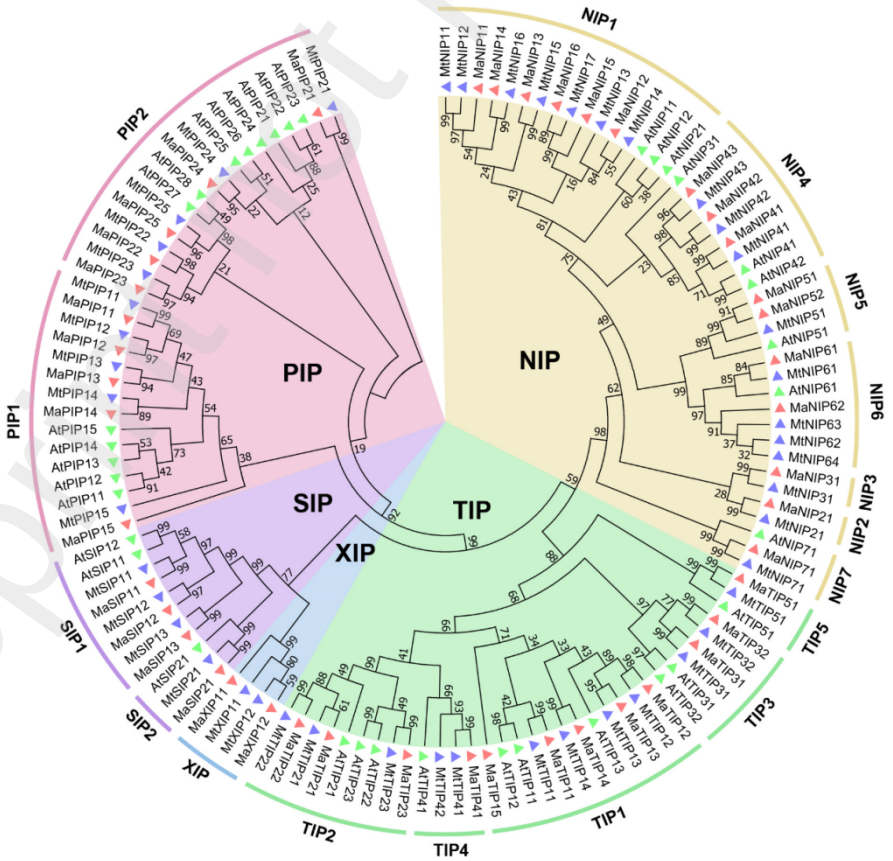

139

Fig. 1. Comparative phylogenetic analysis of AQPs in *M. albus*, *A. thaliana* and *M. truncatula*. The phylogenetic tree was generated by the MEGA7 program. MaAQP, AtAQP, and MtAQP were represented by red, green and blue triangles.

3.2. MaAQP family gene structures and conserved motifs

To elucidate evolutionary patterns within the MaAQP family, a phylogenetic tree based on amino acid sequences was constructed, categorizing MaAQPs into five distinct subgroups (Fig. 2a). To investigate the evolutionary divergence of *MaAQP* genes, we analyzed their gene structures. Members within the same subfamily exhibited high similarity in terms of exon number, exon length, and exon/intron organization (Fig. 2b). 80% (8/10) of *PIP* subfamily genes contained four exons, *TIP* subfamily genes harbored two or three exons, and 87.5% (14/16) of *NIP* subfamily genes had four or five exons. The *SIP* and *XIP* subfamilies contained one to three exons (Fig. 2b).

To explore potential functional differences among MaAQP genes, conserved motif prediction was carried out using the MEME suite, setting the maximum number of detectable motifs at 20. An overview of the 15 conserved motifs identified through MEME analysis is shown (Fig. S1). Motifs 11, 15, 18, and 19 were unique to *PIP* family, motifs 14 and 20 were only found in *TIP* subfamily, motifs 12 and 13 were predominantly present in *NIP* family, and motif 18 was especially cin *SIP* family (Fig. 2c). All MaAQP proteins contained MIP domains, and 95.5% (42/44) MIP domains were distributed on different exons (Fig. 2b).

Critical amino acid residues within MaAQP proteins were identified. The double-NPA motif of *PIP* and *TIP* subfamily is more conserved. Except for MaPIP1;5, both Loop B and Loop E in the *PIP* and *TIP* contained two NPA motifs. The double-NPA motif of *NIP*, *SIP* and *XIP* subfamilies possessed some amino acid substitutions. For instance, the *MaNIP* subfamily contained NPS and NPV sequences. *MaSIP* subfamily included NPT, NPS, NPL and NPI sequences, and *MaXIP* subfamily contained SPV sequence (Table S3).

Further examination of the aromatic/arginine (ar/R) selectivity filter revealed high conservation in the PIP subfamily, where all except MaPIP1;5 shared the "FHTR" signature. In contrast, TIP, NIP, SIP, and XIP families possessed 6, 8, 4, and 1 ar/R filter residues sequence combinations, respectively. Analysis of Froger's positions revealed that PIP, TIP, NIP, SIP, and XIP groups contained 5, 4, 8, 3, and 1 sequence combinations (Table S3).

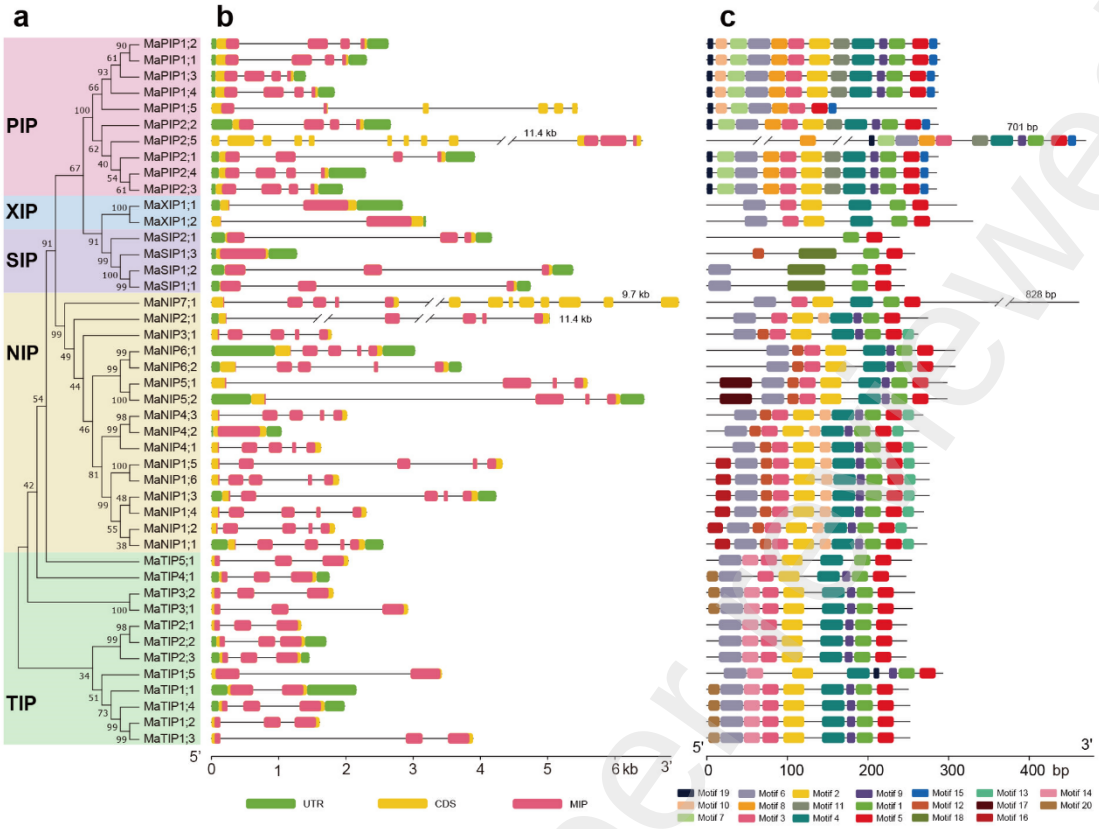

Fig. 2. Evolutionary grouping, structural composition, and conserved motif patterns of MaAQP. (a) Phylogenetic tree of MaAQP proteins generated based on their deduced amino acid sequences. (b) Gene structures of *MaAQP* members were analyzed, with exons and introns represented by yellow boxes and black lines. (c) Conserved motifs were predicted. Each shown as a differently colored box indicating distinct functional elements.

3.3. MaAQP family chromosomal locations and collinearity analysis

A total of 44 *MaAQP* genes were identified and unevenly distributed across 8 chromosomes of *M. albus*. Chromosome 7 contained the highest number of *MaAQP* genes (12, 27.3%), while chromosome 1 contained only 1 (2.3%) *MaAQP* gene (Fig. 3). To identify gene duplication events in, collinearity analysis was performed using OrthoMCL. Fourteen paralogous gene pairs were identified among the *MaAQP* genes (Fig. 3). Duplicated genes were most abundant on chromosome 7, while single duplication gene pairs were found on chromosome 1, 4, 5, and 8 (Fig. 3; Table S4).

The *PIP*, *TIP*, and *NIP* subfamilies contained 8, 4, and 2 paralogous gene pairs, respectively, while no paralogous gene pairs were detected in the *SIP* and *XIP* subfamilies, all paralogous pairs originated within their respective subfamilies (Fig. 5). In addition, Ka/Ks ratio analysis revealed values below 1 for all paralogous pairs, suggesting that these duplicated genes have been subject to purifying selection

throughout the evolution of the *M. albus* genome (Table S4).

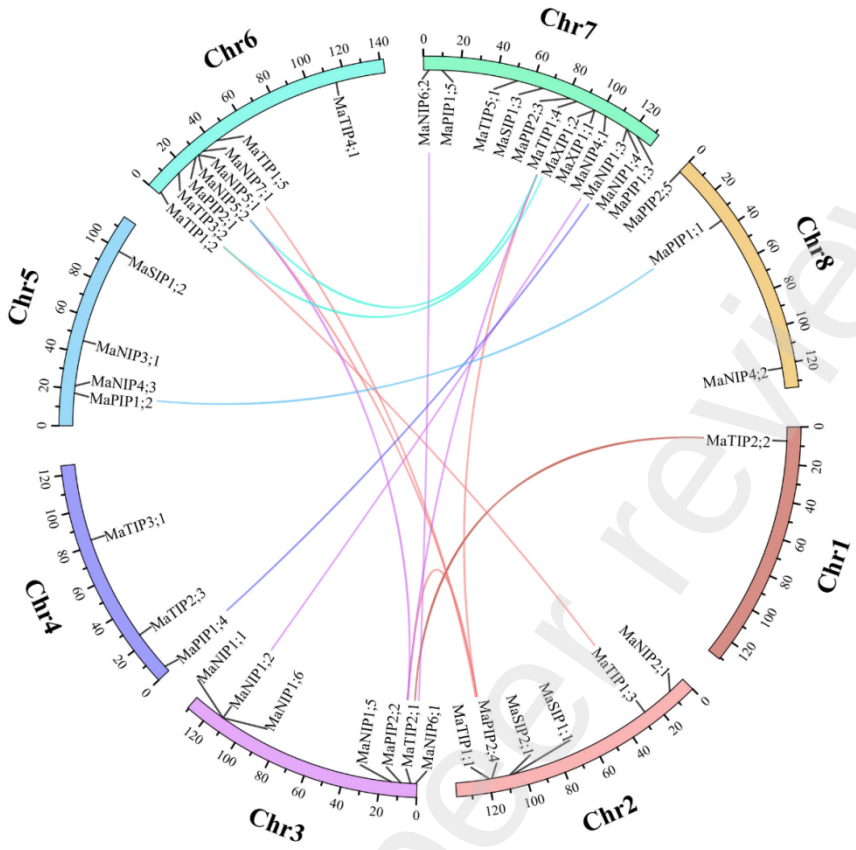

Fig. 3. Chromosomal localization and synteny of duplicated *AQP* genes in *M. albus*. The colored connecting lines indicating syntenic relationships among gene members.

3.4. Identification of cis-elements of MaAQP promoters

Cis-elements within gene promoters serve as binding sites for transcription factors, orchestrating gene expression in a spatial and temporal manner (Yan et al., 2019b). In this study, 20 distinct cis-regulatory elements were identified in the promoter regions of *MaAQP* genes. These elements are predicted to be involved in developmental regulation, responses to abiotic stress, and signaling pathways triggered by various plant hormones (Fig. 4; Table S5). 81.8%, 81.8%, 79.5%, 52.3%, 45.5%, and 40.9% of *MaAQP* genes possessed abscisic acid-responsive elements (ABRE), anaerobic induction elements (ARE), jasmonic acid-responsive elements (TGACG-motif), cis-elements involved in zein metabolism regulation (O2-site), MYB binding sites related to drought inducibility (MBS), and auxin-responsive elements (TGA-element) (Fig. 4a). The *TIP*, *PIP*, and *NIP* groups harbored more cis-acting elements, while the *SIP* and *XIP* families contained fewer. The *NIP* featured the highest count of hormone-related motifs, while stress-responsive elements were more frequently observed in the *PIP* and *TIP* subfamilies. At the chromosomal level, Chr7, Chr6, and Chr2 harbored the largest numbers of phytohormone-

responsive cis-elements (Fig. 4b). Chr7, Chr6, and Chr3 were enriched in stress-related cis-elements, while Chr7, Chr5, and Chr6 harbored the greatest number of development-related cis-elements (Fig. 4c).

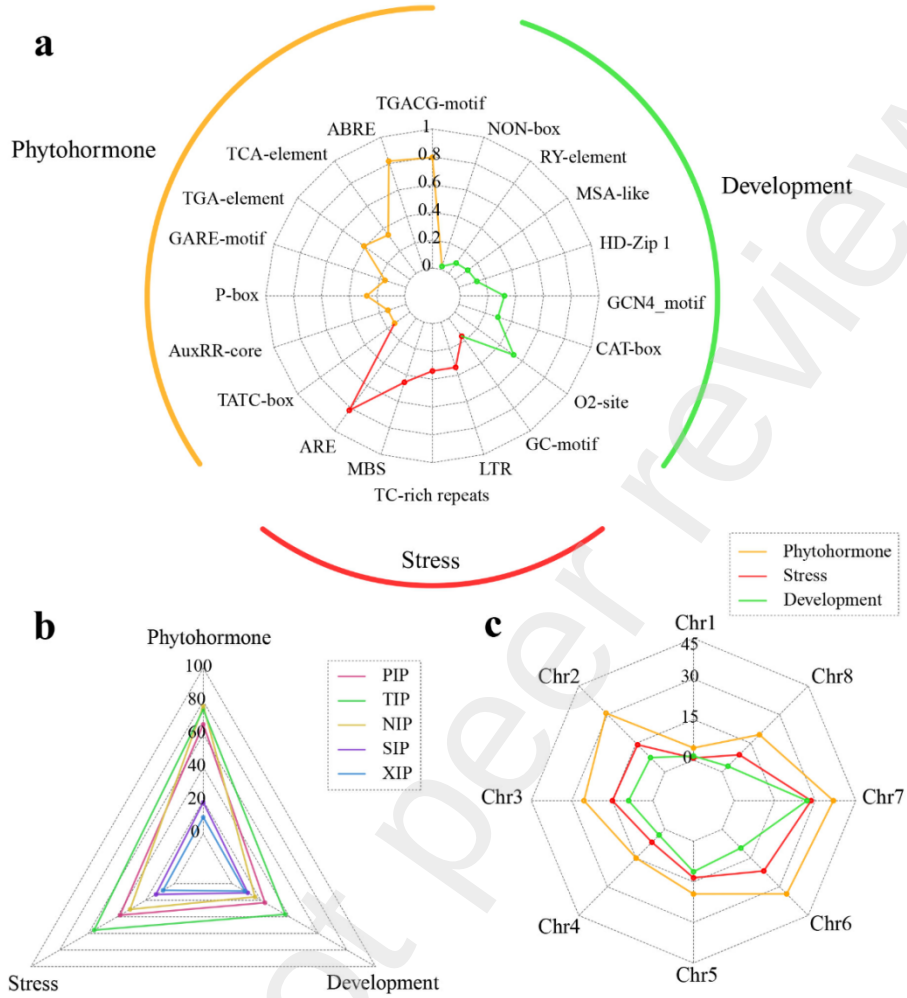

Fig. 4. Cis-element features in *MaAQP* promoter regions.

(a) Proportions of different cis-elements in *MaAQP* genes. (b) Distribution of cis-acting elements in different *MaAQP* subfamilies. (c) Distribution of cis-elements on the *MaAQP* chromosomes

3.5. MaAQP family expression profiles analysis and qRT-PCR validation

To explore the expression patterns of *MaAQP*, we analyzed the transcriptome data of *MaAQP* genes across multiple tissues and under different treatment conditions (Fig. 5; Table S6). The analysis showed that *PIP* subfamily members generally exhibited higher expression levels across conditions. Furthermore, *MaTIP1;2*, *MaTIP1;3*, *MaNIP4;1*, *MaNIP4;3*, and *MaNIP7;1* were specifically expressed in flowers, while *MaTIP3;1*, *MaTIP3;2*, and *MaNIP1;2* showed seed-specific expression. In contrast, *MaNIP3;1* (FPKM < 0.2) and *MaXIP1;2* (FPKM < 0.6) exhibited minimal expression across all tissues and treatments (Fig. 5a). Under salt, drought, and ABA treatments, 1, 4, and 4 *MaAQP* genes were differentially expressed in shoots, whereas 20, 10, and 16 genes responded in roots, respectively. Three

MaAQP genes in roots showed differential expression under salt, drought and ABA treatments (Fig. 5b and c). *MaPIP2;1*, *MaTIP2;2*, and *MaPIP2;1* displayed tissue-specific expression patterns. *MaPIP2;1* was predominantly expressed in the stems and flowers, while *MaTIP2;2* showed high expression in the stems and roots but was downregulated in other tissues. *MaPIP1;1* had the highest expression across all tissues, especially in the roots and stems. These patterns suggest distinct physiological roles for each gene in plant growth and development (Fig. 5d).

The expression patterns of genes from the *PIP* and *TIP* subfamilies with high expression and differential expression folds (*MAPIP2;1*, *MAPIP1;1*, *MAPIP1;5*, and *MaTIP2;2*) were verified by qPCR under drought, salt and ABA treatments. *MaPIP2;1* exhibited a strong induction, with transcript abundance increasing over tenfold in shoots and roots in response to salinity and drought. *MaTIP2;2*, *MaPIP1;1*, and *MaPIP1;5* responded more strongly to salt stress than to drought or ABA treatment. The consistency between qRT-PCR and transcriptome data validates the observed expression trends. (Fig. 6; Table S7).

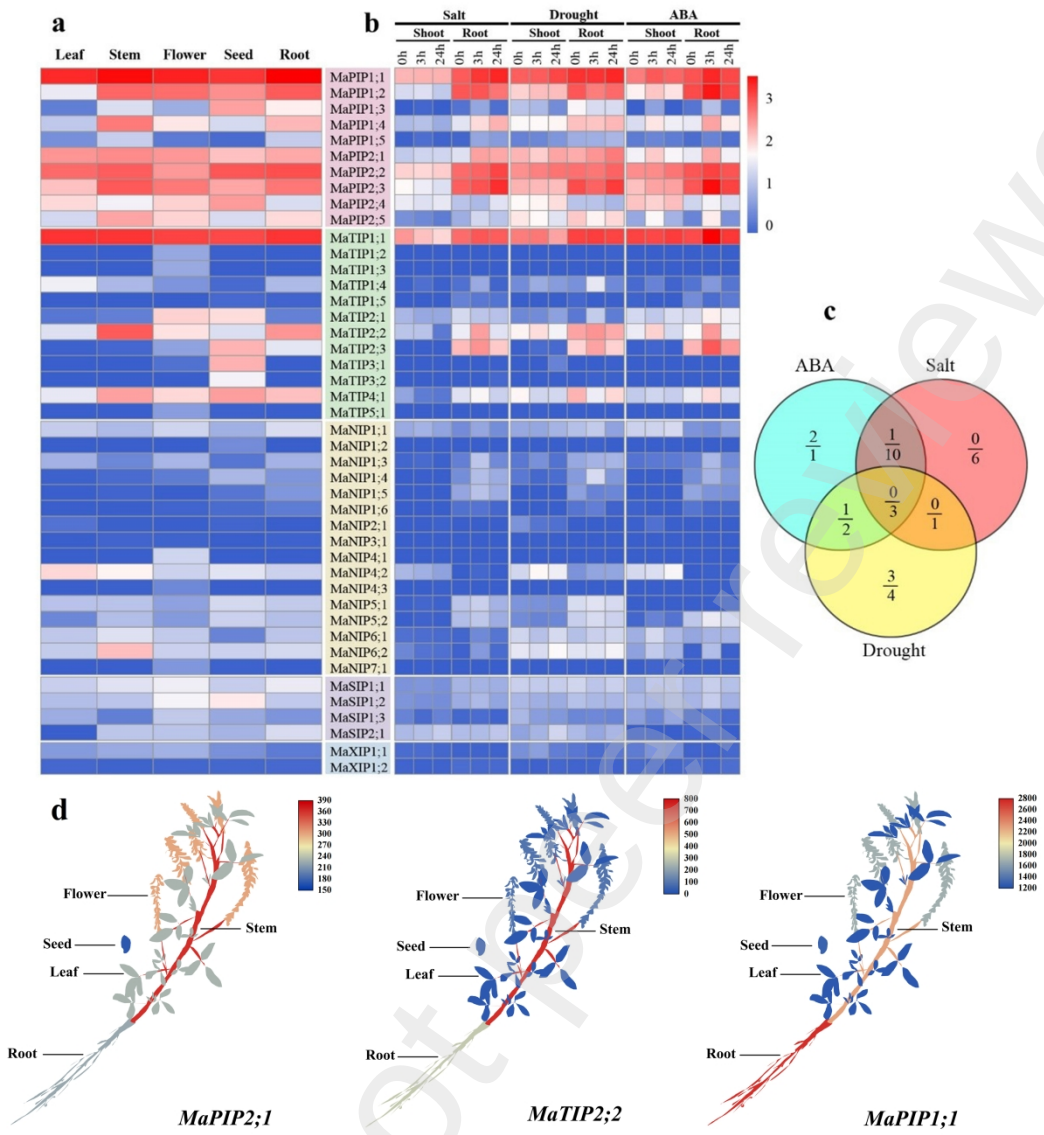

Fig 5. Expression profile of *MaAQP* genes.

(a) Heatmap showing the expression of *MaAQP* across various tissues. (b) Heatmap representation of *MaAQP* under different treatments. Expression values were calculated using $\log_{10}$(FPKM+1) and plotted. (c) Venn diagram illustrating *MaAQP* genes with altered expression under different treatments. Numbers above and below the line represent the *MaAQP* genes from shoots and roots, respectively. (d) Differential expressions of *MaPIP2;1*, *MaTIP2;2*, and *MaPIP1;1* in different organs.

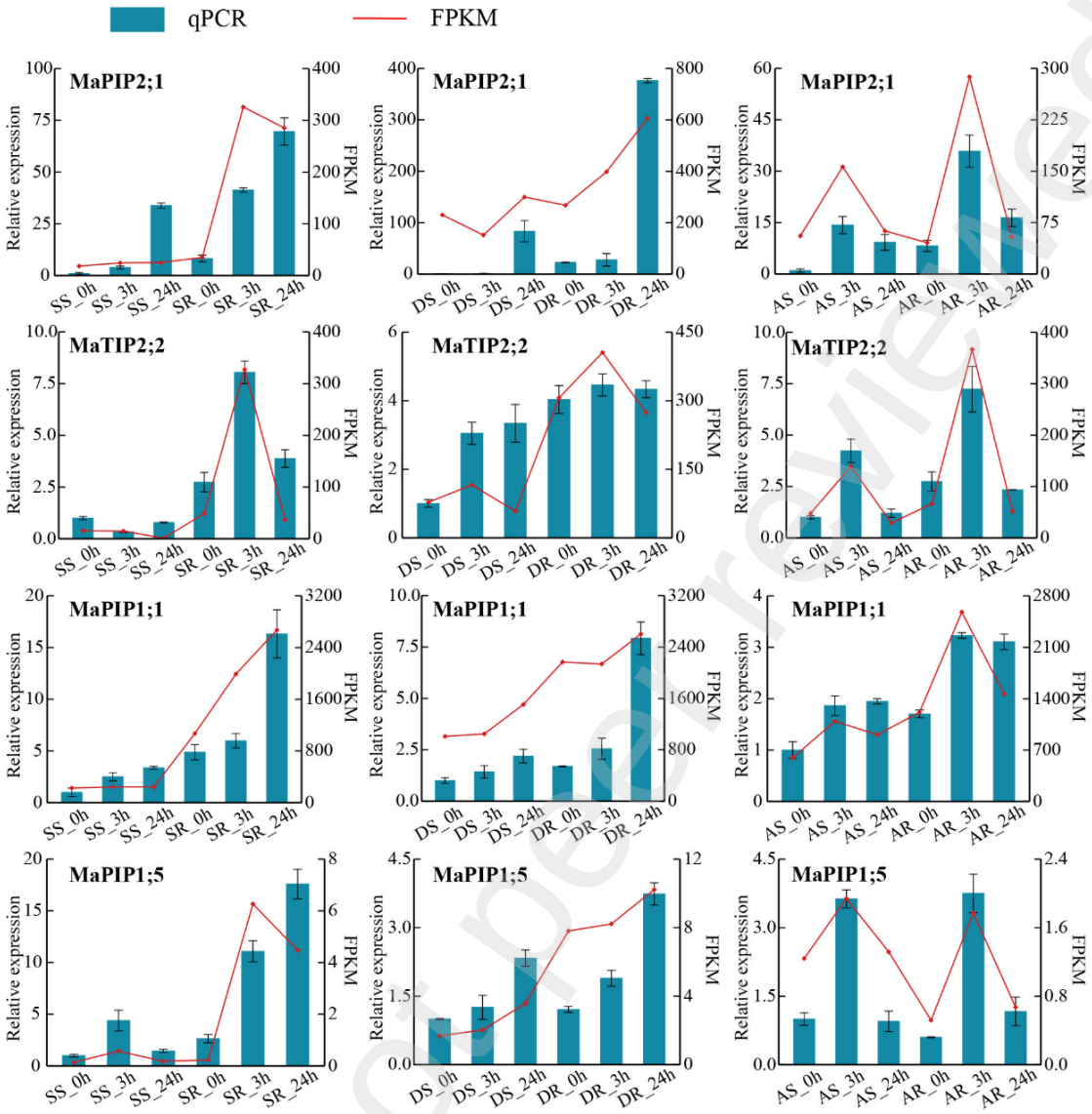

Fig. 6. qPCR validation of *MaAQP* genes expression under salt, drought, and ABA treatments. SS and SR: salt stress in shoots and roots; DS and DR: drought stress in shoots and roots; AS and AR: ABA treatment in shoots and roots.

3.6. Overexpression of MaAQP genes in INVSc1 yeast strains

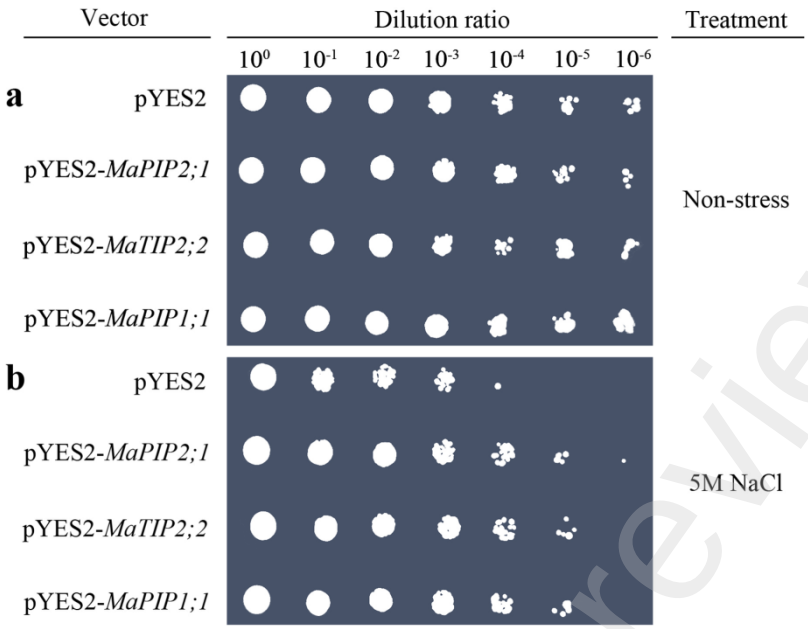

Fig. 7. Growth analysis of INVSc1 yeast cells transformed with *MaAQP* genes under salt stress. (a) Yeast growth under control and (b) salt stress.

To investigate the role of *MaAQP* under salt stress, *MaPIP2;1*, *MaTIP2;2*, and *MaPIP1;1* were selected for yeast genetic transformation and functional assays to evaluate stress tolerance in transgenic yeast strains. *MaPIP2;1*, *MaTIP2;2*, and *MaPIP1;1* cDNAs were amplified with a high-fidelity enzyme, resulting in sizes of 855 bp, 768 bp, and 858 bp. PCR products were ligated into pYES2, transformed into *Escherichia coli*, verified by PCR and sequencing, followed by plasmid extraction and yeast cell transformation. (Fig. S2). Under control conditions, yeast strains overexpressing *MaPIP2;1*, *MaTIP2;2*, and *MaPIP1;1* exhibited growth similar to yeast transformed with the empty pYES2 vector (Fig. 7a). Under salt stress, the yeast harboring the empty vector failed to grow at a dilution of 10^{-5}, whereas yeast strain expressing *MaPIP2;1*, *MaTIP2;2*, and *MaPIP1;1* formed visible colonies at this dilution. Notably, the strain expressing *MaPIP2;1* continued to show growth even at a dilution of 10^{-6}. In addition, the colony sizes of yeast expressing the *MaAQP* genes were larger than those of the control strain in the presence of salt, suggesting that overexpression of these genes improved salt resistance in yeast (Fig. 7b).

3.7. Overexpression of MaAQP genes enhances salt stress tolerance in M. albus

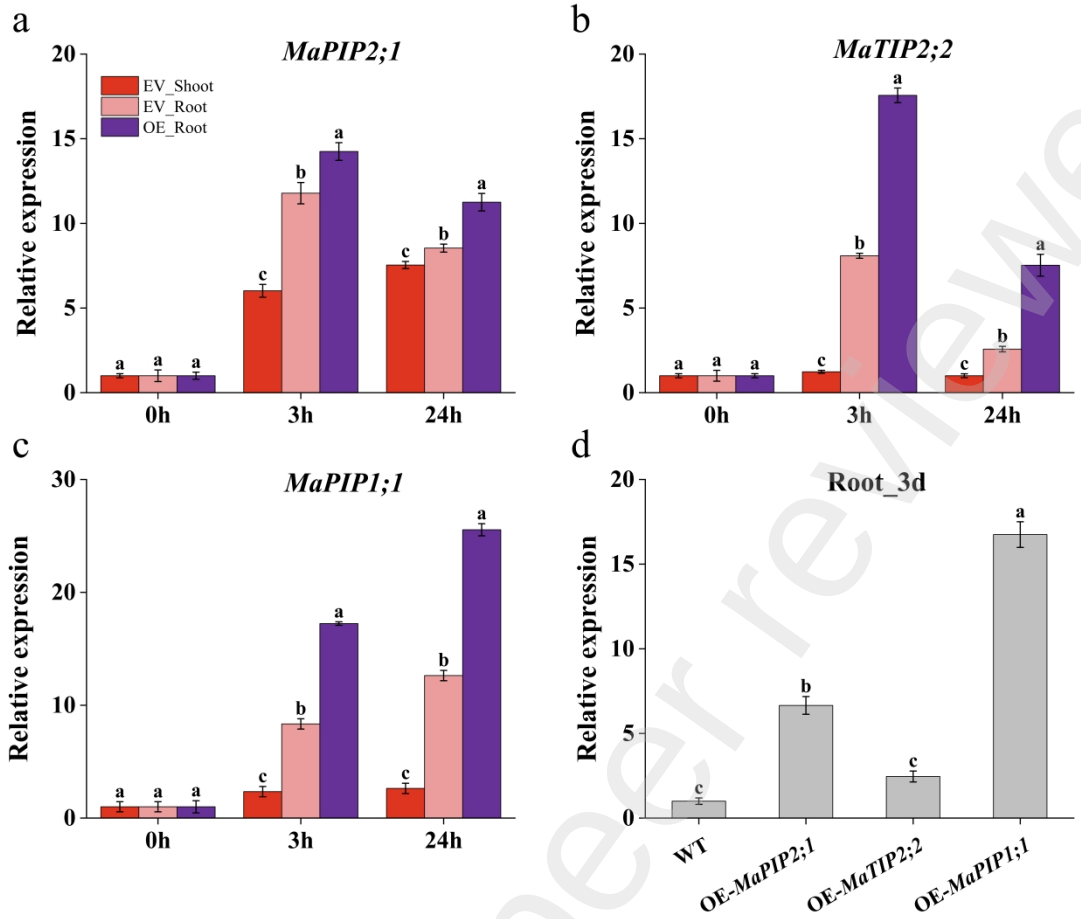

Fig. 8. *MaAQP* expression in *M. albus* under NaCl treatment.

(a–c) Relative expression of *MaPIP2;1*, *MaTIP2;2*, and *MaPIP1;1* in shoots and roots at 0 h, 3 h, and 24 h after NaCl treatment. (d) Expression in roots after 3 days of NaCl treatment.

To validate the level of *MaPIP2;1*, *MaTIP2;2*, and *MaPIP1;1* under NaCl treatment, qRT-PCR was performed on empty vector (EV) and overexpression (OE) lines, which were derived from root hair transformation. Samples were collected at 0 h, 3 h, and 24 h, in both shoots and roots (Fig. 9a-c). The results showed that *MaPIP2;1* had the highest expression in roots at 3 h, with significantly elevated levels in the OE lines (Fig. 9a). Similarly, *MaTIP2;2* exhibited strong expression in roots, particularly at 3 h, and the OE lines showed increased expression (Fig. 9b). For *MaPIP1;1*, expression was higher in roots than in shoots, peaking at 24 h in the OE lines (Fig. 9c). After 3 days of NaCl treatment, all *MaAQP* genes were significantly upregulated in the roots of the OE lines compared to EV (Fig. 9d). These results suggest that *MaAQP* genes, especially *MaPIP2;1*, are vital for water transport in *M. albus*, and their expression is further enhanced by overexpression under NaCl stress.

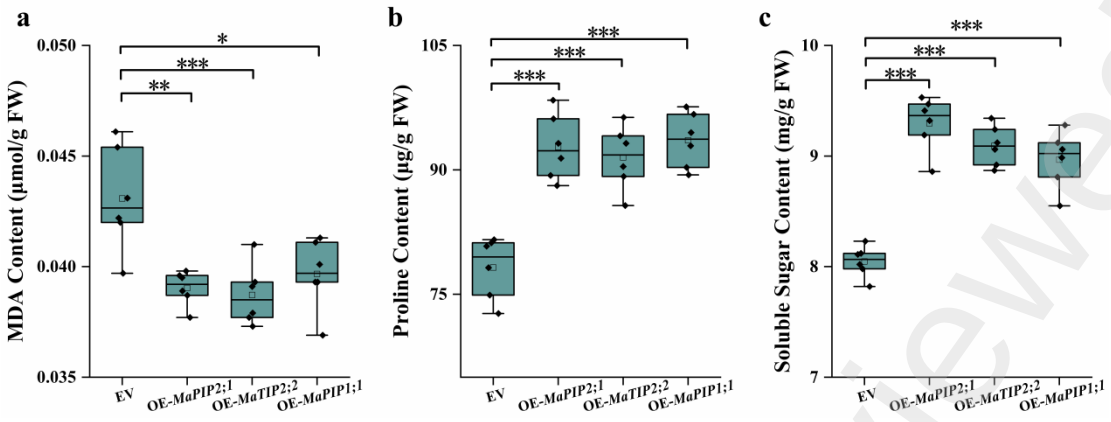

Fig. 9. Physiological responses of *M. albus* root hair transformants to salinity. (a) MDA, (b) proline, and (c) soluble sugar levels in transgenic hair roots after 3 days of NaCl treatment.

The overexpression of *MaPIP2;1*, *MaTIP2;2*, and *MaPIP1;1* in *M. albus* resulted in improved physiological responses under salt stress compared to the EV. MDA content was significantly reduced in all transgenic hair roots, suggesting a reduction in oxidative stress. The reduction in MDA was most pronounced in the OE-*MaTIP2;2* and OE-*MaPIP2;1* lines, highlighting their superior ability to mitigate oxidative damage under saline conditions (Fig. 9a). Proline levels were markedly higher in all transgenic roots than in EV. Among these, the OE-*MaPIP2;1* line exhibited the highest accumulation of proline, indicating its enhanced capacity for osmotic adjustment (Fig. 9b). Similarly, soluble sugar content was also notably elevated in all transgenic roots. OE-*MaPIP2;1* accumulated the highest levels of soluble sugars, further emphasizing its superior ability to regulate osmotic pressure (Fig. 9c). The data show that overexpression of *MaPIP2;1*, *MaTIP2;2*, and *MaPIP1;1* improves the ability of *M. albus* to withstand salt stress, mainly through alleviating oxidative damage and enhancing osmotic regulation. Among the three, the MaPIP2;1 overexpression line exhibited the most notable physiological improvements, suggesting its crucial involvement in boosting salt resistance in *M. albus*. (Fig. 9).

4. Discussion

AQPs are membrane channel proteins essential for cellular water balance, especially in environments with high salinity or restricted water availability. (Siemens and Zwiazek, 2003). Since their discovery in 1993, AQPs with MIP domains have been characterized in various plant species, including rice (Sakurai et al., 2005), soybean (Deshmukh et al., 2013), barley (Hove et al., 2015), and maize (Chaumont et al., 2001). In this study, 44 *MaAQP* genes were identified in *M. albus*, a number comparable to that in alfalfa (46) (Min et al., 2019) and banana (47) (Hu et al., 2015), and higher than that in *Arxabidopsis* (35) (Johanson et al., 2001) and *Vicia sativa* (21) (Wei et al., 2019). Phylogenetic

analysis revealed that these MaAQP proteins could be categorized into five conserved subfamilies, aligning with previous classifications in related species (Zhang et al., 2013; Min et al., 2019). The basic characteristics of MaAQP, such as their molecular weight, isoelectric point, and hydrophobicity, were largely consistent with other known AQP proteins (Fujiyoshi et al., 2002). Predicted subcellular localization suggests that the majority of MaAQP members associate with either the plasma membrane or vacuolar membrane, although experimental validation will be required for confirmation.

Gene structure diversity is a fundamental driver of gene family evolution (Hao et al., 2010). In *MaAQP* genes, members of each subfamily generally share similar exon counts and exon–intron layouts. Most *TIP*, *SIP*, and *XIP* genes contain one to three exons, while most of the *PIP* and *NIP* genes contain four or five. Exceptions include *MaPIP2;5* and *MaNIP7;1*, which contain 12 and 13 exons, respectively (Fig. 2b). Conserved sequence elements were largely consistent among genes grouped by evolutionary proximity, while each subfamily displayed distinct element arrangements, reflecting functional and structural divergence. For instance, *MaPIP2;5* and *MaNIP7;1* possessed distinct motifs and longer non-domain sequences, compared to other members of their respective subfamilies, suggesting that their extended CDS and amino acid sequences may contribute to specialized functions (Min et al., 2019). 95.5% of the MIP domains in *MaAQP* genes were distributed across multiple exons (Fig. 2b), indicating that the domain evolution is closely coupled with gene structural evolution. *AQP* are known to mediate the transport of water as well as various neutral solutes. These functions are closely linked to specific structural domains, including the NPA region, ar/R selectivity site, and Froger's positions (Kammerloher et al., 1994; Hove and Bhave, 2011). Conserved sequence elements related to substrate selectivity are prominent in PIP members, while greater sequence variability is present among TIP and NIP groups (Table S3). This divergence may underline the greater functional diversity reported in TIP and NIP members (Cao, 2017). Additionally, the Froger's residues of the PIP1 and PIP2 subtypes were mainly "ESAFW" and "QSAFW" (Table S3), which could explain the functional differences in water transport activity between hese two subtypes.

Gene duplication contributes significantly to family expansion and functional variation (Yan et al., 2019a). In the *MaAQP* family, the *PIP*, *TIP*, and *NIP* subgroups contain 8, 4, and 2 pairs of paralogous genes, respectively, and all paralogous pairs are confined within their respective subfamilies (Table S4). This pattern suggests that the PIP and TIP subfamilies have experienced more extensive expansion than the NIP, SIP, and XIP subfamilies. Their broader expansion may suggest a higher degree of functional

significance, aligning with findings from related studies (Kadam et al., 2017; Reddy et al., 2017).

Sequences located upstream of coding regions contribute to transcriptional regulation through interactions with regulatory proteins. (Yan et al., 2019b). Regulatory sequences upstream of *MaAQP* coding regions were examined, and most contained elements linked to developmental processes, hormone sensitivity, and environmental adaptability (Fig. 4). Prior studies have demonstrated that *AQP* genes respond high salt concentration and water deficiency (Liu et al., 2013; Thakral et al., 2023), are regulated by hormones such as ABA (Lin et al., 2007), and play roles in processes like fruit ripening (Cao et al., 2024), which aligns with the regulatory features identified in this study.

To further explore the relationship between *AQP* genes and plant growth, development, hormone signaling, and responses to salinity, their transcript levels were examined across multiple tissues and experimental conditions. Overall, genes from the *PIP* subfamily exhibited higher expression levels than those from other subfamilies. Notably, *MaTIP1;2* and *MaTIP1;3* showed strong flower-preferential expression, implying a role in floral processes, while *MaTIP3;1*, *MaTIP3;2*, and *MaNIP1;2* showed seed-specific expression, indicating possible involvement in seed germination (Fig. 5). Additionally, qPCR was conducted for four *MaAQP* genes including *MaPIP2;1*, *MaPIP1;1*, *MaPIP1;5*, and *MaTIP2;2*. These genes showed high transcript abundance and notable changes under stress conditions. The results indicated that *MaPIP1;1*, *MaPIP1;5*, and *MaTIP2;2* had greater fold increases in response to salt treatment compared to drought and ABA, while *MaPIP2;1* maintained strong induction across all three conditions (Fig. 6).

To assess functional relevance, heterologous expressions of *MaPIP2;1*, *MaTIP2;2*, and *MaPIP1;1* in yeast confirmed their role in improving tolerance to salt stress. Transgenic yeast expressing these genes showed enhanced growth under salt conditions compared to controls, supporting their involvement in osmotic regulation. This aligns with previous findings in tobacco, where overexpression of *NtPIP1* improved salt resistance and water-use efficiency (Mahdieh et al., 2008). Taken together, our findings provide a comprehensive characterization of the *MaAQP* family in *M. albus*, demonstrating their structural diversity, regulatory complexity, and potential functional roles in response to abiotic stress.

Organ-specific transcriptome data revealed that *MaPIP2;1*, *MaTIP2;2*, and *MaPIP1;1* exhibit distinct tissue-specific expression patterns in *M. albus*, indicating functional divergence among *AQP* family members. *MaPIP2;1* was predominantly expressed in the stem and flower, while *MaTIP2;2* showed higher expression in the stem and root. In contrast, *MaPIP1;1* was highly expressed across all

tissues. These patterns suggest that each gene may contribute to water transport or regulation in a tissue-dependent manner. PIP2 isoforms are commonly associated with efficient water permeability in aerial organs (Shivaraj et al., 2021), consistent with the expression of *MaPIP2;1*. TIPs, such as *MaTIP2;2*, are localized to the tonoplast and are essential for vacuolar water homeostasis, particularly under osmotic stress (Li et al., 2022). The general expression pattern of *MaPIP1;1* suggests involvement in maintaining basal water flow across various organs. These findings enhance our understanding of tissue-specific expression patterns of *MaAQP* genes and offer valuable context for future research. Notably, *MaPIP2;1* exhibited the greatest increase in osmoprotectants, which is in line with the role of PIP2 aquaporins in facilitating water transport and mediating stress adaptation. PIP2 isoforms, particularly in aerial organs, are known to facilitate efficient water transport, a function that was supported by the high expression of *MaPIP2;1* in the stem and flower. In contrast, the overexpression of *MaTIP2;2* and *MaPIP1;1* contributed to the reduction in oxidative damage and enhanced stress tolerance, with *MaPIP2;1* showing the most pronounced effect. These findings suggest that the *MaAQP* genes, especially *MaPIP2;1*, are essential for maintaining water homeostasis, reducing oxidative stress, and promoting osmotic protection under salt stress.

The qRT-PCR results and physiological assays confirm that overexpression of *MaPIP2;1*, *MaTIP2;2*, and *MaPIP1;1* significantly enhances salt stress tolerance in *M. albus* (Fig. 8 and 9). The transgenic roots showed a significant reduction in MDA content, indicating a decrease in oxidative damage, while the increased proline and soluble sugar content suggested enhanced osmotic adjustment under NaCl stress (Fig. 9). These results are consistent with recent studies where overexpression of aquaporin genes improved salt tolerance by reducing oxidative stress and regulating osmotic homeostasis (Neri et al., 2024; Wei et al., 2024).

5. Conclusion

In conclusion, we performed a comprehensive analysis of the *M. albus AQP* family, identifying 44 *MaAQP* genes which were categorized into five subfamilies: *PIP*, *TIP*, *NIP*, *SIP*, and *XIP*. Phylogenetic, gene structure, and conserved motif analyses provided valuable insights into evolutionary relationships and functional diversification of MaAQP proteins. Transcriptome profiling, along with qPCR validation, further supported the significant involvement of *MaAQP* genes in the plant's response to salt stress. Functional validation through yeast overexpression and transgenic *M. albus* plants demonstrated that *MaPIP2;1*, *MaTIP2;2*, and *MaPIP1;1* enhanced salt tolerance. The transgenic plants showed improved

salt tolerance by reducing oxidative damage, as evidenced by lower MDA content, and promoting osmotic adjustment through increased proline and soluble sugar levels. The results clarified *AQP* function in leguminous species and supported future efforts to strengthen forage and crop resilience to salinity.

Author contributions

J.Y.Z. conceived and designed this study; X.F.Z. and C.B.Z. performed the experiments; X.F.Z. and Z.J.X. analyzed the data. Z.J.X. and X.F.Z wrote the manuscript. J.Y.Z. revised the manuscript.

Acknowledgments

This work was financially supported by the National Natural Science Foundation of China (U23A200216, 32271752), Inner Mongolia Seed Industry Science and Technology Innovation Major Demonstration Project (2022JBGS0040), Principal Scientist Responsbility Project of Gansu Province (23ZDKA013) and the Fundamental Research Funds for the Central Universities (lzujbky-2022-ey17).

Data availability statement

All data, tables and figures in this manuscript are original.

Declaration of competing interest

The authors declare no conflicts of interest.

References

Bensmihen, S., Rippa, S., Lambert, G., Jublot, D., Pautot, V., Granier, F., Giraudat, J., Parcy, F., 2002. The homologous ABI5 and EEL transcription factors function antagonistically to fine-tune gene expression during late embryogenesis. The Plant Cell, 14: 1391–1403.

Cao, R.Z., 2017. Genome-wide identification of aquaporin family and the transient expression assay system setup of mesophyll protoplasts in wheat. M.D. Northwest A & F University.

Cao, Y., Lv, J., Tai, R., Tang, W., Ge, Y., 2024. Impacts of 1-methylcyclopropene (1-MCP) and ethephon treatments on expression of aquaporin (*AQP*) genes during apple fruit ripening. Scientia Horticulturae, 331: 113126.

Carles, C., Bies-Etheve, N., Aspart, L., Léon-Kloosterziel, K.M., Koornneef, M., Echeverria, M., Delseny, M., 2002. Regulation of *Arabidopsis thaliana Em* genes: role of *ABI5*. The Plant Journal, 30: 373–383.

Chaumont, F., Barrieu, F., Wojcik, E., Chrispeels, M.J., Jung, R., 2001. Aquaporins constitute a large and highly divergent protein family in *Zea mays*. Plant Physiology, 125(3): 1206–1215.

Chen, C., Wu, Y., Li, J., Wang, X., Zeng, Z.H., Xu, J., Liu, Y.L., Feng, J.T., Chen, H., He, Y.H., Xia, R., 2023. TBtools-II: A ‘‘one for all, all for one’’ bioinformatics platform for biological big-data mining. Molecular Plant, 16(11): 1733–1742.

Chen, J., Nolan, T.M., Ye, H., Zhang, M., Tong, H., Xin, P., Chu, J., Chu, C., Li, Z., Yin, Y., 2017. Arabidopsis WRKY46, WRKY54, and WRKY70 transcription factors are involved in brassinosteroid-regulated plant growth and drought responses. The Plant Cell, 29: 1425–1439.

Chen, K., Li, G.J., Bressan, R.A., Song, C.P., Zhu, J.K., Zhao, Y., 2020. Abscisic acid dynamics, signaling, and functions in plants. Journal of Integrative Plant Biology, 62: 25–54.

Chen, M., Penfield, S., 2018. Feedback regulation of COOLAIR expression controls seed dormancy and flowering time. Science, 360: 1014–1017.

Chrispeels, M.J., Maurel, C., 1994. Aquaporins: the molecular basis of facilitated water movement through living plant cells?. Plant Physiology, 105(1): 9.

Deshmukh, R.K., Vivancos, J., Guérin, V., Sonah, H., Labbé, C., Belzile, F., Bélanger, R.R., 2013. Identification and functional characterization of silicon transporters in soybean using comparative genomics of major intrinsic proteins in *Arabidopsis* and *Oryza sativa*. Plant Molecular Biology, 83(4): 303–315.

Fujiyoshi, Y., Mitsuoka, K., De Groot, B.L., Philippsen, A., Grubmüller, H., Agre, P., Engel, A., 2002. Structure and function of water channels. Current Opinion in Structural Biology, 12(4): 509–515.

Hao, Y.J., Song, Q.X., Chen, H.W., Zou, H.F., Wei, W., Kang, X.S., Ma, B., Zhang, W.K., Zhang, J.S., Chen, S.Y., 2010. Plant NAC-type transcription factor proteins contain a *NARD* domain for repression of transcriptional activation. Planta, 232(5): 1033–1043.

Hove, R.M., Bhave, M., 2011. Plant aquaporins with non-aqua functions: deciphering the signature sequences. Plant Molecular Biology, 75(4): 413–430.

Hove, R.M., Ziemann, M., Bhave, M., 2015. Identification and expression analysis of the barley (*Hordeum vulgare* L.) aquaporin gene family. PLoS One, 10(6): e0128025.

Hu, W., Hou, X., Huang, C., Yan, Y., Tie, W., Ding, Z., Wei, Y., Liu, J., Miao, H., Lu, Z., Li, M., Xu, B., Jin, Z., 2015. Genome-wide identification and expression analyses of aquaporin gene family during development and abiotic in banana (*Musa acuminata*). International Journal of Molecular Sciences, 16(8): 19728–19751.

Javot, H., Maurel, C., 2002. The role of aquaporins in root water uptake. Annals of Botany, 90(3): 301–313.

Johanson, U., Karlsson, M., Johansson, I., Gustavsson, S., Sjövall, S., Fraysse, L., Weig, A.R., Kjellbom, P., 2001. The complete set of genes encoding major intrinsic proteins in *Arabidopsis* provides a framework for a new nomenclature for major intrinsic proteins in plants. Plant Physiology, 126(4): 1358–1369.

Kadam, S., Abril, A., Dhanapal, A.P., Koester, R.P., Vermerris, W., Jose, S., Fritschi, F.B., 2017. Characterization and regulation of aquaporin genes of sorghum [*Sorghum bicolor* (L.) Moench] in response to waterlogging stress. Frontiers in Plant Science, 8: 862.

Kammerloher, W., Fischer, U., Piechottka, G.P., Schäffner, A.R., 1994. Water channels in the plant plasma membrane cloned by immunoselection from a mammalian expression system. The Plant Journal, 6(2): 187–199.

Kawasaki, S., Borchert, C., Deyholos, M., Wang, H., Brazille, S., Kawai, K., Galbraith, D., Bohnert, H.J., 2001. Gene expression profiles during the initial phase of salt stress in rice. The Plant Cell, 13(4): 889–905.

Li, Q., Tong, T., Jiang, W., Cheng, J., Deng, F., Wu, X., Chen, Z.H., Ouyang, Y., Zeng, F., 2022. Highly conserved evolution of aquaporin PIPs and TIPs confers their crucial contribution to flowering process in plants. Frontiers in Plant Science, 12: 761713.

Liu, C., Fukumoto, T., Matsumoto, T., Gena, P., Frascaria, D., Kaneko, T., Katsuhara, M., Zhong, S., Sun, X., Zhu, Y., Iwasaki, I., Ding, X., Calamita, G., Kitagawa, Y., 2013. Aquaporin *OsPIP1;1* promotes rice salt resistance and seed germination. Plant Physiology and Biochemistry, 63: 151–158.

Maathuis, F.J.M., Filatov, V., Herzyk, P., Krijger, G.C., Axelsen, K.B., Chen, S., Green, B.J., Li, Y., Madagan, K.L., Sánchez-Fernández, R., Forde, B.G., Palmgren, M.G., Rea, P.A., Williams, L.E., Sanders, D., Amtmann, A., 2003. Transcriptome analysis of root transporters reveals participation of multiple gene families in the response to cation stress. The Plant Journal, 35(6): 675–692.

Mahdieh, M., Mostajeran, A., Horie, T., Katsuhara, M., 2008. Drought stress alters water relations and expression of *PIP*-type aquaporin genes in *Nicotiana tabacum* plants. Plant and Cell Physiology, 49(5): 801–813.

Maurel, C., Verdoucq, L., Luu, D.T., Santoni, V., 2008. Plant aquaporins: membrane channels with multiple integrated functions. Annual Review of Plant Biology, 59: 595–624.

Min, X., Wu, H., Zhang, Z., Wei, X., Jin, X., Ndayambaza, B., Wang, Y., Liu, W., 2019. Genome-wide identification and characterization of the aquaporin gene family in *Medicago truncatula*. Journal of Plant Biochemistry and Biotechnology, 28(3): 320–335.

Neri A., Francini A., Giovannelli A., Traversari S., Sebastiani L., 2024. Differences in mineral and osmotic balances enhance zinc translocation in an aquaporin overexpressing poplar. Environmental and Experimental Botany, 208: 108528.

Reddy, P.S., Tharanya, M., Sivasakthi, K., Srikanth, M., Hash, C.T., Kholova, J., Sharma, K.K., Vadez, V., 2017. Molecular cloning and expression analysis of aquaporin genes in pearl millet [*Pennisetum glaucum* (L.) R. Br.] genotypes contrasting in their transpiration response to high vapour pressure deficits. Plant Science, 265: 167–176.

Rogers, M.E., Colmer, T.D., Frost, K., Henry, D., Cornwall, D., Hulm, E., Deretic, J., Hughes, S.R., Craig, A.D., 2008. Diversity in the genus *Melilotus* for tolerance to salinity and waterlogging. Plant and Soil, 304(1): 89–101.

Sakurai, J., Ishikawa, F., Yamaguchi, T., Uemura, M., Maeshima, M., 2005. Identification of 33 rice aquaporin genes and analysis of their expression and function. Plant and Cell Physiology, 46(9): 1568–1577.

Shivaraj, S.M., Sharma, Y., Chaudhary, J., Rajora, N., Sharma, S., Thakral, V., Ram, H., Sonah, H., Singla-Pareek, S.L., Sharma, T.R., Deshmukh, R., 2021. Dynamic role of aquaporin transport system under drought stress in plants. Environmental and Experimental Botany, 186: 104437.

Siemens, J.A., Zwiazek, J.J., 2003. Effects of water deficit stress and recovery on the root water relations of trembling aspen (*Populus tremuloides*) seedlings. Plant Science, 165(1): 113–120.

Thakral, V., Sharma, Y., Mandlik, R., Kumawat, S., Patil, G., Sonah, H., Isenring, P., Bélanger, R., Sharma, T.R., Deshmukh, R., 2023. Identification of *VrNIP2-1* aquaporin with novel selective filter regulating the transport of beneficial as well as hazardous metalloids in mungbean (*Vigna radiata* L.). Plant Physiology and Biochemistry, 203: 108057.

Walz, T., Hirai, T., Murata, K., Heymann, J.B., Mitsuoka, K., Fujiyoshi, Y., Smith, B.L., Agre, P., Engel, A., 1997. The three-dimensional structure of aquaporin-1. Nature, 387(6633): 624–627.

Wang, S.S., Duan, Z., Zhang, J.Y., 2021. Establishment of hairy root transformation system of *Melilotus albus* induced by *Agrobacterium rhizogenes*. Acta Agrestia Sinica, 29(11): 2591–2599.

Wei H., Ruan J., Zhou R., Bai Y., Liu M., Jiang F., Wu Z., 2024. Screening and Verification of Aquaporin Gene AsPIP1-3 in Garlic (*Allium sativum* L.) under Salt and Drought Stress. Horticulturae, 10(7): 738.

Wei, X.Y., Jin, X.Y., Ndayambaza, B., Min, X.Y., Zhang, Z.S., Wang, Y.R., Liu, W.X., 2019. Transcriptome-wide characterization and functional identification of the aquaporin gene family during drought stress in Vicia sativa. DNA and Cell Biology, 38(5): 123–134.

Wu, F., Duan, Z., Xu, P., Yan, Q., Meng, M., Cao, M., Jones, C.S., Zong, X., Zhou, P., Wang, Y., Luo, K., Wang, S., Yan, Z., Wang, P., Di, H., Ouyang, Z., Wang, Y., Zhang, J., 2022. Genome and systems biology of *Melilotus albus* provides insights into coumarins biosynthesis. Plant Biotechnology Journal, 20(3): 592–609.

Yan, Q., Wu, F., Ma, T., Zong, X., Ma, Q., Li, J., Zhao, Y., Wang, Y., Zhang, J., 2019b. Comprehensive analysis of bZIP transcription factors uncovers their roles during dimorphic floret differentiation and stress response in *Cleistogenes songorica*. BMC Genomics, 20(1): 760.

Yan, Q., Wu, F., Yan, Z., Li, J., Ma, T., Zhang, Y., Zhao, Y., Wang, Y., Zhang, J., 2019a. Differential co-expression networks of long non-coding RNAs and mRNAs in *Cleistogenes songorica* under water stress and during recovery. BMC Plant Biology, 19(1): 23.

Zhang, D.Y., Ali, Z., Wang, C.B., Xu, L., Yi, J.X., Xu, Z.L., Liu, X.Q., He, X.L., Huang, Y.H., Khan, I.A., Trethowan, R.M., Ma, H.X., 2013. Genome-wide sequence characterization and expression analysis of major intrinsic proteins in soybean (*Glycine max* L.). PLoS One, 8(2): e56312.

Zhang, M.X., Bai, R., Nan, M., Ren, W., Wang, C.M., Shabala, S., Zhang, J.L., 2022. Evaluation of salt tolerance of oat cultivars and the mechanism of adaptation to salinity. Journal of Plant Physiology, 273: 153708.

Zhao, C., Zhang, H., Song, C., Zhu, J.K., Shabala, S., 2020. Mechanisms of plant responses and adaptation to soil salinity. The Innovation, 1(1): 100017.